Full Length Article

Optimization of heavy crude oil recovery using oil-soluble catalyst precursor under electromagnetic heating

Arash Tajik [a,*], Temurali Kholmurodov [a,b], Yasser I. I. Abdelsalam [a], Nafis A. Nazimov [c], Alexey V. Vakhin [a,*]

[a] *Institute of Geology and Oil & Gas Technologies, Kazan Federal University, Kazan 420008, Russia*
[b] *Department of Chemistry, Samarkand State University, 140104 Samarkand, Uzbekistan*
[c] *PJSC «TATNEFT» named after V.D. Shashin, 75 Lenin St., Almetyevsk, 423450*

A B S T R A C T

In order to improve the heavy oil quality, the electromagnetic (EM) heating method with the addition of metal catalysts has been considered. Oil-soluble catalyst precursors, which consist of a ligand and a metal, prevent their clumping and precipitation by dispersing nanoparticles in oil. Unfortunately, no research was found to investigate the effect of adding this type of catalyst on increasing the efficiency of EM heating and optimizing the recovery of heavy oil. The aim of this paper was to propose nickel-adipic (NOSC) as an oil-soluble catalyst precursor to increase the efficiency of EM heating. A set of 2.45 GHz industrial magnetrons was used as the microwave radiation source with the addition of 1 wt% NOSC (containing 0.39 % Ni) at time intervals of 3, 6 and 9 min. At 9 min, asphaltene and resin content decreased by 21.91 % and 40.07 %, and saturate and aromatic content increased by 11.13 % and 41.3 %, respectively. In addition, the viscosity also showed a decrease of about 60 %. Elemental analysis showed 11 %, 13 % and 20 % reduction of sulfur after 3, 6 and 9 min, respectively. According to the results of GC–MS, the content of n-C_{26}–C_{32} compared to the control sample (ACO) was reduced by 2 times in 6 min. In addition, observing the increase in the content of naphthalenes and light alkylbenzenes in aromatic compounds was a proof of the effectiveness of the NOSC catalytic system in heavy oil upgrading. This paper presents a promising approach to enhance the performance of EM heating in heavy crude oil recovery.

1. Introduction

Nowadays, the need for energy resources is increasing rapidly with the technological advancement and population growth [1–3]. Nearly 70 % of the world's oil reserves are heavy crude oil (HCO) and bitumen. In general, HCO because of high viscosity and presence of heteroatoms in its composition has many technical and economic problems [4–6]. The thermal methods can be introduced as one of the most widely used techniques in reducing the viscosity and improving HCO quality [7–10]. The purpose of conventional thermal oil recovery methods is to improve HCO recovery by increasing reservoir temperature, removing heavy compounds and reducing oil viscosity. Aqueous thermal recovery such as fire flooding, hot water injection, steam injection and steam assisted gravity drainage (SAGD) is known as one of the most common thermal methods of HCO recovery [11,12]. Unfortunately, environmental and economic limitations, as well as incompatibility with specific types of HCO reservoirs, such as deep reservoirs, heterogeneous formations, etc.,
can create challenges for these methods.

Recently, the electromagnetic (EM) heating technique has been considered to solve these challenges [13,14]. Ritchey [15] first proposed this method in 1956. Microwaves are EM waves with a frequency range of 300 MHz to 300 GHz, which corresponds to wavelengths of 1 mm to 1 m [16]. Current research shows that using EM heating can resulted in saving a significant amount of energy and time [17–20].

The EM heating can be described as polar molecules absorb microwave radiation and oscillate, and due to these fluctuations at the molecular level, EM radiation is converted into heat energy.

It is obvious that, the excessive presence of asphaltenes and resins is one of the most important factors in the high viscosity of HCO [21,22]. Thereby, these compounds, due to their dielectric properties, have a high ability to absorb microwave radiation compared to aromatic and saturated compounds. Hence, by absorbing microwave radiation, the temperature of the reservoir increases and the heat produced is gradually distributed through other dielectric materials in the system.

[17,23,24]. On the other hand, the absorption of microwave radiation by asphaltene and resin molecules leads to the formation of hot spots at the molecular level. The created hot spots cause cracking and removal of long chain molecules or their conversion into smaller chain molecules [25,26]. It is evident that the result of all these interactions is a reduction in viscosity and an increase in the recovery efficiency of HCO.

This is apparent that the role of nanoparticles in reducing the viscosity of HCO during EM heating and other thermal methods is very essential to improve oil mobility. Significant research has been carried out in the field of nanocatalysts in the thermal recovery of HCO and viscosity reduction [27–32]. In particular, this type of catalyst has raised the recovery efficiency due to the high surface to volume ratio which has the ability to create more contact surface with the surrounding environment of HCO [33]. Li et al. [34] studied the upgrading of HCO by carbon nanocatalysts under microwave irradiation. They concluded that carbon nanocatalysts could increase oil recovery efficiency at 150 °C. Also, carbon nanocatalysts diminish viscosity and the time required to recover HCO compared to conventional methods. Vakhin et al. [35] conducted research based on the use of EM heating in the presence of iron–based nanoparticles. They believed that the presence of iron-based nanoparticles under microwave treatment had a significant effect on breaking and converting high–molecular weight compounds to light–molecular weight compounds, as well as reducing the viscosity of HCO. The time parameter plays a key role in EM heating, because if during this process, the heating rate does not match with time, Probability of losing light oil compounds and increasing viscosity is extremely high. Taheri Shakib et al. [36] used nanoparticles of titanium oxide (TO), super active carbon (CA) and iron (Fe), under microwave radiation for different time periods of 2, 4, 6, 8 and 10 min. The results obtained from the experiments showed that the CA had a considerable effect in reducing the viscosity within 6 min due to having the highest capacity to absorb microwaves. Moreover, the highest amount of desulfurization in 6 min was done by CA nanoparticles.

One of the disadvantages of using metals and their oxides is the lack of dissolution and accumulation in HCO. This phenomenon reduces the efficiency of the catalytic system [37,38]. Accordingly, researchers have proposed the use of oil-soluble catalytic systems as a solution to this problem. In general, oil-soluble catalysts consist of an organic ligand such as carboxylic acids and transition metals. The mechanism of this type of catalytic system is that metal is dispersed in oil by an organic ligand, so that it prevents from accumulating and clumping [39–42].

Fan et al.[43] showed in their research that both types of catalysts soluble in water and oil have the ability to facilitate the aquathermolysis of crude oil. Temurali Khalmrodov et al. [42] by developing an oil-soluble nanocatalytic system, reported a decrease in viscosity and an acceptable increase in the ratio of hydrogen to carbon using the aquathermolysis method.

By reviewing the research conducted in the field of HCO recovery by thermal methods, unfortunately no attention has been paid to the simultaneous use of oil soluble catalysts and EM heating technique [40,44–48]. Therefore, nickel–adipate as an oil-soluble catalyst precursor was proposed to improve the performance of EM heating. Adipic acid is an organic ligand and its advantages include easy accessibility, economical and environmentally friendly. Moreover, different time intervals were suggested to detailed review the effectiveness of the catalytic system. To present the results, experiments such as viscosity measurement, Fourier transform infrared (FTIR), scanning electron microscope (SEM), spectrometer (EDX), Group Composition SARA, elemental analysis, X-ray diffraction (XRD) and gas chromatography–mass spectrometry (GC–MS) were performed.

2. Experimental sections

2.1. Materials

Adipic acid, Nickel (II) nitrate hexahydrate, NaOH, ethanol, methanol, n–hexane, and toluene were obtained from Sigma Company. The HCO sample was selected the Ashalcha heavy crude oil (ACO) field from the Republic of Tatarstan (Russia). The chemical and physical properties of ACO are shown in Table 1.

2.2. Synthesis of NOSC

The experimental setup includes a beaker, a dropping funnel, and a mechanical stirrer, all maintained at room temperature. This arrangement allows for the controlled addition of reagents and efficient mixing, ensuring the successful formation of the desired NOSC product. In order to prepare NOSC, Adipic acid and Nickel (II) nitrate hexahydrate were dissolved separately in a 1:2 M ratio in ethanol and mixed for 1 h. The pH of the adipic acid + ethanol solution was adjusted to 9 by using sodium hydroxide. Then, the solution of Nickel (II) nitrate hexahydrate + ethanol was added drop by drop and stirred for 2 h. Consequently, the precipitates were washed with ethanol and water to remove excess ligand and metal salt. The obtained NOSC was dried at the room temperature for 18 h.

2.3. Sample preparation and experiment procedure

The samples containing 20 g of ACO and 2 wt% of catalyst precursor (containing 0.39 % nickel) were prepared to investigate the effect of the oil soluble catalyst precursor using EM heating in 3, 6, and 9 min. The heating was no more than 70 °C in order to study the influence of the microwave field. For this purpose, the chamber was cooled and microwave irradiation was interrupted every 1 min. A schematic of the microwave apparatus used in this study is shown in Fig. 1.

A set of industrial magnetrons with a frequency of 2.45 GHz was used as a source of microwave radiation. The transmission of radiation from a set of magnetrons to the reactor is carried out using a waveguide path. Finally, the abbreviated nomenclature of the samples during this study is shown in Table 2.

2.4. Analytical procedures

2.4.1. SEM and EDX analysis

Merlin field emission scanning electron microscope (Carl Zeiss) equipped with AZtec X-Max energy dispersive spectrometer (Oxford Instruments) was used. Spectrometer resolution 127 eV. To reduce the possible error of EDX analysis, the working distance of 9 mm and the accelerator voltage of 20 kV were selected.

2.4.2. XRD analysis

With the aim of investigating the phase composition and structure of NOSC, the phase composition and structure of NOSC, a Shimadzu XRD–7000S automatic powder diffractometer (Kyoto, Japan) was used. X-ray diffraction was performed with 40 kW scanning voltage and 40 mA current through Cu Kα radiation. The scanning angle was in the range of 5-90° 2θ and with a speed of 5°/min.
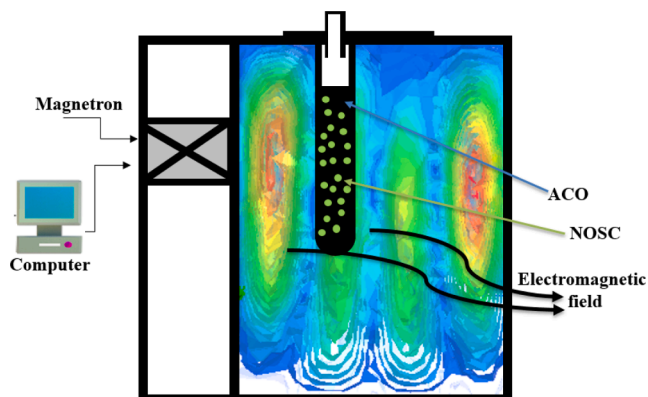
2.4.3. SARA analysis

According to ASTM D2007 standards, the oil samples were divided into four groups: saturated, aromatic, resin and asphaltene. The oil/n–hexane mixture was prepared in a ratio of 1:40. After 12 h, asphaltenes were separated from maltene by filtration. A glass chromatographic column (20x 500 mm) filled with Al_2O, that was previously calcined at 450 °C for 3.5 h, was used to separate maltenes.

2.4.4. Viscosity measurements

After completing the EM heating process, the samples were placed at room temperature for 24 h to stabilize. The viscosity of ACO and samples containing NOSC at different times was measured and analyzed by Fungilab AlphaL viscometer (Valencia, Spain) at 20 °C. TL5 spindle was used to measure samples. The amount of oil needed to evaluate the

Table 1
Physical and chemical information of ACO.

Viscosity at 20 ℃ (mPa × s)	Density (g × cm⁻³)	API gravity	Elemental content (%)					SARA analysis (%)			
			C	H	N	S	O	saturates	aromatics	resins	asphaltenes
2950	0.973	13.8	82.02	11.52	0.45	5.77	0.24	27.39	31.14	34.81	6.66

Fig. 1. Schematic of the microwave device used for EM heating of the ACO.

Table 2
The samples under investigation in brief.

Number	Samples	Conditions
1	ACO	Ashalcha Heavy Crude Oil
2	blank –3 min	ACO without catalyst precursor During 3, 6 and 9 min under EM heating
3	blank –6 min	
4	blank –9 min	
5	NOSC –3 min	ACO with catalyst precursor During 3, 6 and 9 min under EM heating
6	NOSC –6 min	
7	NOSC –9 min	

viscosity was 6.7 ml. Data were gathered when the spring torque was in the range of 60–90 %. It should be noted that the maximum relative error of the equipment was assumed about 1 %.

2.4.5. Elemental analysis

Elemental composition including carbon, hydrogen, nitrogen, oxygen, and sulfur present in oil and samples after EM heating treatment were analyzed. Then the H/C ratio was calculated for each sample according to the data.

2.4.6. FTIR analysis

FT–IR spectroscopy measurements to identify functional groups of the catalyst and samples before and after treatment (ACO, asphaltenes and, resins), using a Bruker Tensor II FTIR infrared spectrometer in the wavelength range of 400 and 4000 cm − 1 were performed.

2.4.7. GC–MS analysis

Chromatic-Crystal 5000 gas chromatography with ISQ detector (USA) was used to examine the fraction of saturated and aromatic compounds. The sample volume was 0.1 Âμl. Chromatography was performed in linear temperature programming mode from 60 °C to 280 °C. Mass spectrum data processing was done using Xcalibur program.

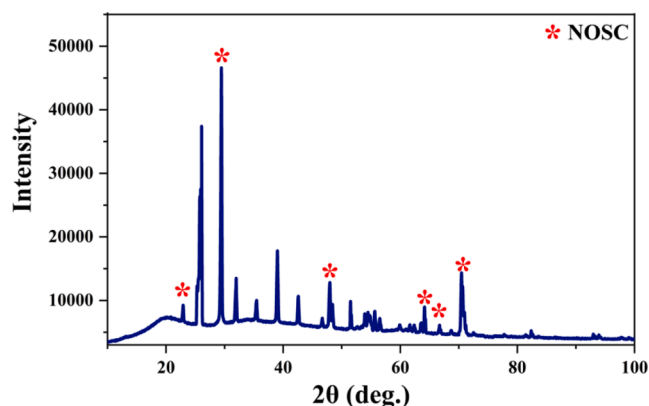## 3. Results and discussion

3.1. Characterization of NOSC

3.1.1. XRD and FT-IR spectroscopy results

In order to confirm the formation of the complex, XRD and FT-IR analysis were performed.

XRD analysis showed the possibility of forming a complex between nickel and Adipic acid due to the presence of new peaks at 23, 30, 48, 64, 67 and 70 (2θ) (Fig. 2). According to the literature, carboxylic acid groups show four main peaks in FTIR spectra: 3300–2500 cm⁻¹ (O–H stretching), 1760 cm⁻¹ (C=O stretching), 1440–1395 cm⁻¹ (O–H bending) and 1210–1320 cm⁻¹ (C–O stretch). Fig. 3 shows that the peaks corresponding to 3300–2500 cm⁻¹ (O–H stretching), 1440–1395 cm⁻¹ (O–H bending) and 1210–1320 cm⁻¹ (C–O stretching) undergo significant changes with the formation of NOSC. These changes indicate the involvement of carboxylic acid groups in the complexation process, which is consistent with the successful synthesis of NOSC through metal carboxylate ion interactions. [41,49]. The sharp peak at 3573 cm⁻¹ in the NOSC spectrum is due to the free OH group of ethanol [50].

3.1.2. SEM and EDX analysis

As seen in Fig. 4, SEM and EDX techniques were performed to analyze the morphology, size and elemental composition of the NOSC. According to the results, the size of most NOSC particles is almost less than 100 nm. The specific surface area of these nanoparticles is increased due to the quasi–spherical structure (surface to volume ratio). It is predicted that increasing the specific surface area and the compaction of nanoparticles can enhance the probability of random collision between oil molecules and catalyst. It has also been proven that nanoparticles with smaller sizes have a great ability to absorb EM radiation and propagate heat transfer efficiency [51]. Moreover, the main elements of carbon (58.03 %), oxygen (26.97 %), and nickel (13.97 %) were observed in the EDX data analysis (Fig. 4c). The identification of oxygen and carbon elements can be argued by their presence in adipic acid structure. The available impurities originate from the materials necessary for the analysis preparation. Finally, a purity of ≈99 % can be considered for NOSC due to the high content of Ni, C and O elements. Due to the high content of carbon, nickel and oxygen elements, 99 %≈ purity is not far from expected for NOSC. Also, the location and ratio of different elements of EDX analysis were presented in the supplementary
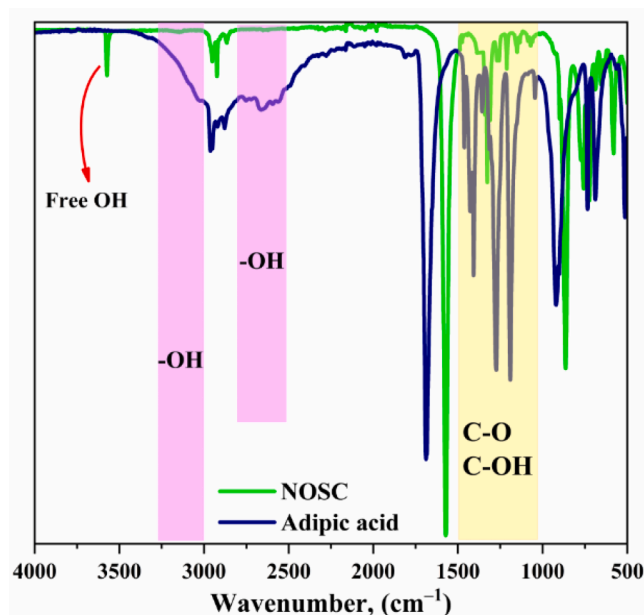

Fig. 2. XRD patterns of synthesized NOSC.

Fig. 3. FT-IR spectra of Adipic acid and NOSC.

3.2. Upgrading of ACO under EM heating by NOSC

This study was designed with the aim of optimizing the recovery of heavy oil using oil-soluble catalyst precursor under EM heating. The improvement of ACO quality was evaluated by analytical methods such as Group Composition (SARA) analysis, viscosity, FT-IR spectroscopy, elemental analysis and GC–MS.

3.2.1. Group composition (SARA) of ACO after EM heating treatment

Fig. 5 shows the results of SARA for samples with and without NOSC in 3, 6, and 9 min compared to ACO.

All samples under EM heating show acceptable reduction of asphaltene contents. The highest amount of asphaltene reduction is related to NOSC–9 min with 26.88 %. The decreasing trend of resin content was observed in all samples. The maximum reduction is related to NOSC–9 min about 40 %. Obviously, due to the presence of O, N and S elements in asphaltenes and resins, they have a high ability to absorb microwaves. The rotation of polar molecules placed in an alternating EM field has a significant effect on increasing the efficiency of EM heating [52]. The high dielectric properties of polar compounds cause large carbon molecules to crack and break during treatment. In addition, the phenomenon of secondary cracking also occurs with the formation of a hot zone [53]. Note that, during the cracking of asphaltene and resin due to the high thermal conductivity of the oil, the lighter compounds contents will also change. Of course, based on many studies, it can be concluded that the rate of conversion of heavy compounds into light
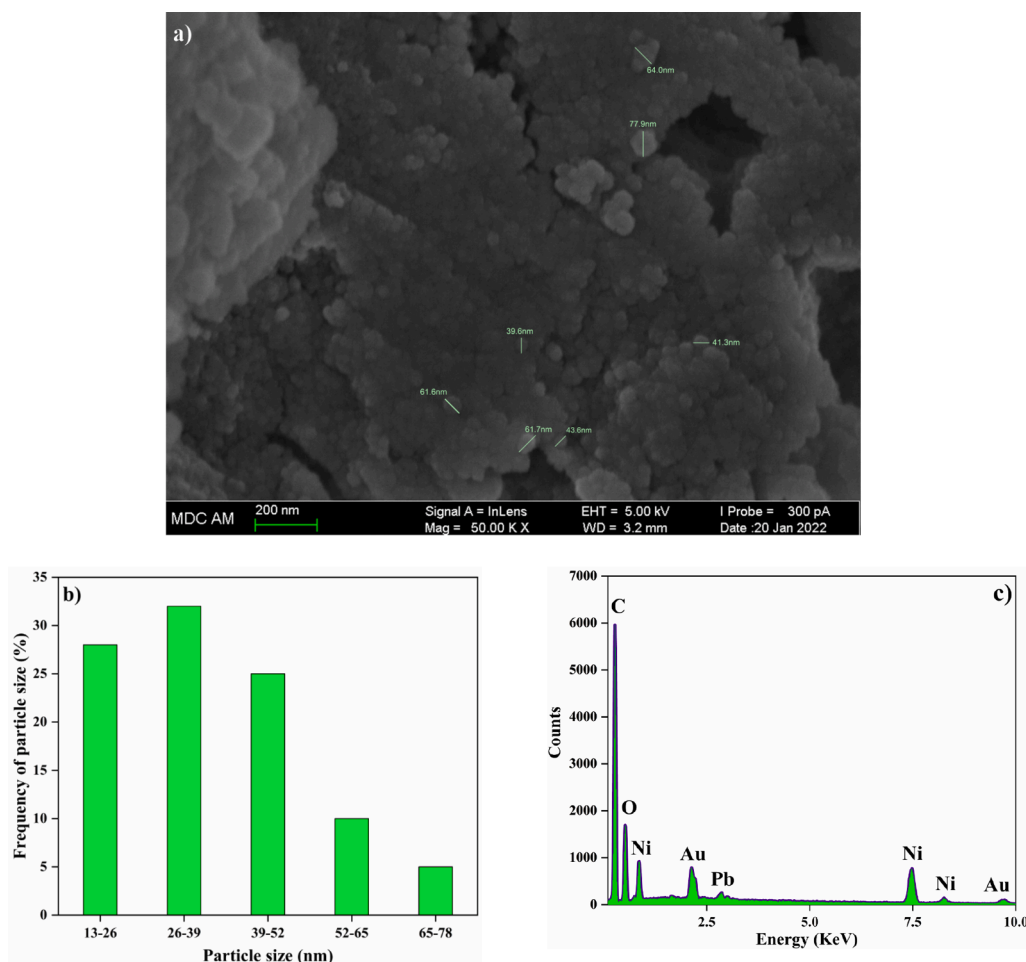

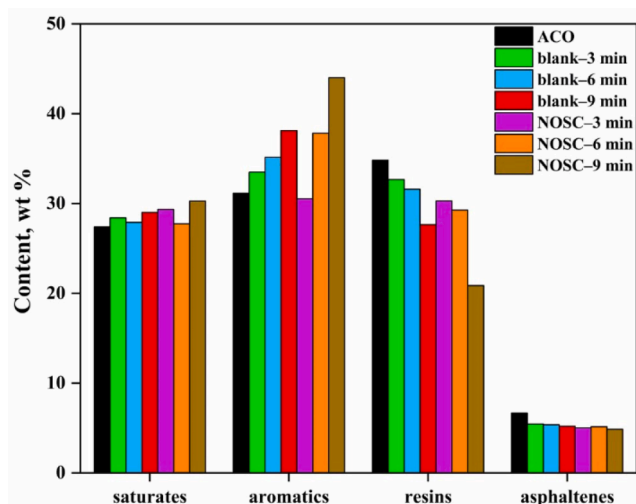**Fig. 4.** SEM images (a), the nanoparticle size frequency (b), and EDX analysis (c) of NOSC.

Fig. 5. Group Composition (SARA) of ACO after EM heating treatment.

compounds is higher than the rate of light compounds losing. According to the results, with the increase of heating time, the amount of saturation and aromatic compounds increased, that the highest increase in saturate and aromatic content by NOSC–9 min was 10.5 % and 41.3 % respectively. On the other hand, the increase of saturation and aromatic compounds after 9 min for the sample without catalyst was 5.95 % and 22.41 %, respectively. Moreover, the content of resins decreased by 20.55 % and asphaltenes by 21.77 %. From the above data, it can be concluded that the presence of NOSC during EM heating has a significant effect in reducing the content of heavy compounds and increasing light compounds. It is assumed that, these increases in contents originated from the cracking of long–chain hydrocarbons and the conversion of them to shorter–chain hydrocarbons.

3.2.2. ACO viscosity reduction after EM heating treatment

The viscosity diagram of ACO and samples with and without catalyst in 3, 6, and 9 min (T=20C and different shear rate) intervals are presented in Fig. 6.

According to the obtained data, the viscosity of crude oil diminished in all samples. Changes were not noticeable for samples without NOSC. On the other hand, the samples containing the catalyst showed promising results, so that the maximum viscosity reduction of about 60 % was

Fig. 6. Dynamic viscosity of ACO under EM heating treatment with Different shear rates at 20°C.

observed for NOSC–9 min.Asphaltenes and resins due to their polar nature have a high capacity to absorb microwave radiation [54]. The presence of nickel nanoparticles along with these compounds creates a wider range of hot zones. As a result, more cracking and breaking occurs, and the viscosity reduction increases [55]. In addition, many free radicals are also produced during these interactions, which, because of their high instability, have a high potential for polymerization and produce long chain compounds. It is predicated that, the use of oil-soluble catalyst precursor prevents the formation of these polymer compounds and can guarantee the irreversibility of viscosity.

3.2.3. Elemental analysis of ACO after EM heating treatment

The composition of ACO elements (CHNOS), before and after exposure to EM heating in the presence of NOSC was shown in Table 3.

According to the results that in all samples, the amount of oxygen increased compared to ACO after treatment. It is assumed that this increase is due to the presence of air during the experiment and the provision of conditions for the oxidation process. Meanwhile, with the passage of time, the amount of oxygen showed a downward trend. It can be concluded that with the increase of irradiation time, the effect of oxidation reactions has decreased. Also, desulfurization was observed in all samples after EM heating, and the highest amount of desulfurization corresponding to NOSC–9 min was 20.28 wt%. There are several theories about the cause of the decrease in sulfur content. Firstly, sulfur has a high potential to absorb microwave radiation. Hence, it is affected to a greater extent [17,56]. This hypothesis can be clearly seen in blank samples. Secondly, due to the creation of hot zones in the area of asphaltene and resin accumulation, the possibility of breaking C–S bonds is very high [57]. Thirdly, the catalyst acts by weakening the π bonds between asphaltenes molecules and also by breaking the C–S bonds and prevents their aggregation [58]. By comparing the blank and NOSC samples, it can be seen that with the presence of NOSC, the desulfurization process occurred to a greater extent. The nitrogen values have also decreased due to the property of absorbing microwave radiation. In addition, the ratio of hydrogen to carbon in the sample containing NOSC increased compared to blank and ACO, and in the meantime, NOSC–9 min has recorded the highest value with an increase of 8.97 %. It is worth mentioning that increase in the H/C ratio could be attributed to the breaking of multiple carbon–carbon bonds, cracking, reducing the content of large asphaltene and resin molecules, and increase of saturate and aromatic content. It is worth mentioning that, increase in H content indicates that a hydrogenation reaction is likely occurring upon EM heating. Heavy oil molecules undergo a series of reactions called hydrocracking by splitting the hydrocarbon chain and breaking the C–C, C–S, C–O and C–N bond, as well as hydrogenating olefins during the hydrogenation reaction, which increases the content of saturated hydrocarbons[59–61]. In general, by comparing the data, it can be concluded that the presence of NOSC and the increase in the duration of radiation, as complementary factors, have led to an acceptable improvement in the quality of ACO.

3.2.4. NOSC morphology and EDX analysis after EM heating

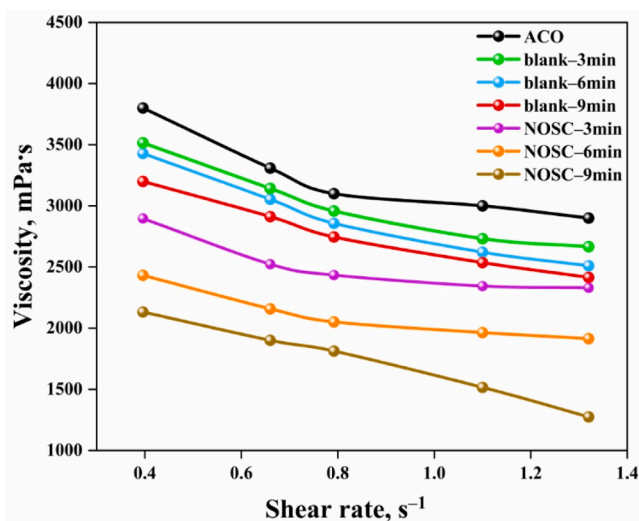By means of SEM and EDX analysis, the possible changes in the size,

Table 3
Elemental composition of ACO after EM heating experiments.

Elemental Analysis (wt.%)						
	C	H	N	S	O	H/C
ACO	82.02	11.52	0.45	5.77	0.24	1.673
blank–3 min	82.10	11.33	0.44	5.72	0.41	1.644
blank–6 min	82.13	11.56	0.43	5.63	0.25	1.676
blank–9 min	82.16	11.72	0.43	5.42	0.27	1.698
NOSC–3 min	82.60	11.49	0.40	5.10	0.41	1.656
NOSC–6 min	82.40	11.93	0.36	5.01	0.30	1.724
NOSC–9 min	82.18	12.61	0.29	4.6	0.32	1.828

composition and morphology of NOSC particles after the EM heating process were analyzed and shown in Figs. 7 and 8. In all samples, with the passage of treatment time, the nanoparticles kept their spherical shape and compactness, and on the other hand, the size of these particles has increased Fig. 7. This phenomenon can occur due to the absorption of microwaves by nickel, which leads to the collapse of the particles and the formation of Ni_xS_y. [62].

In EDX analysis, all samples contained some elemental sulfur as shown in Fig. 8 and the maximum sulfur content was observed for NOSC–9 min of approximately 8 %.

It should be noted that the location and ratio of different elements of EDX analysis were presented in the supplementary information section (Figs. S2 – S4 and Tables S2 – S4).

3.2.5. XRD analysis

The XRD patterns of solids remaining after EM heating at 3, 6, and 9 min are presented in Fig. 9.

Significant amounts of Ni_xS_y (x = 2.548,7,9 and y = 2, 6, 8) appeared in different peaks, indicating the effective role of NOSC in the
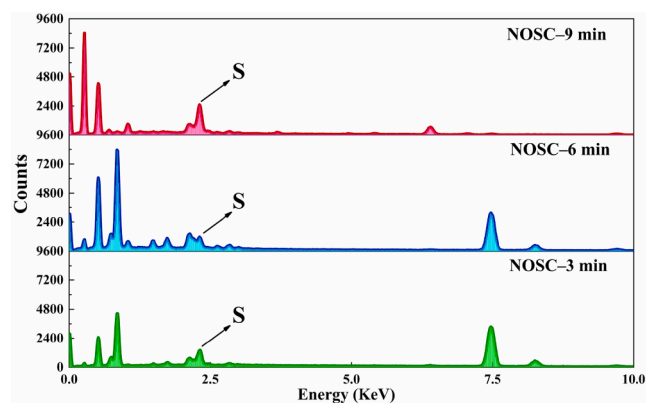

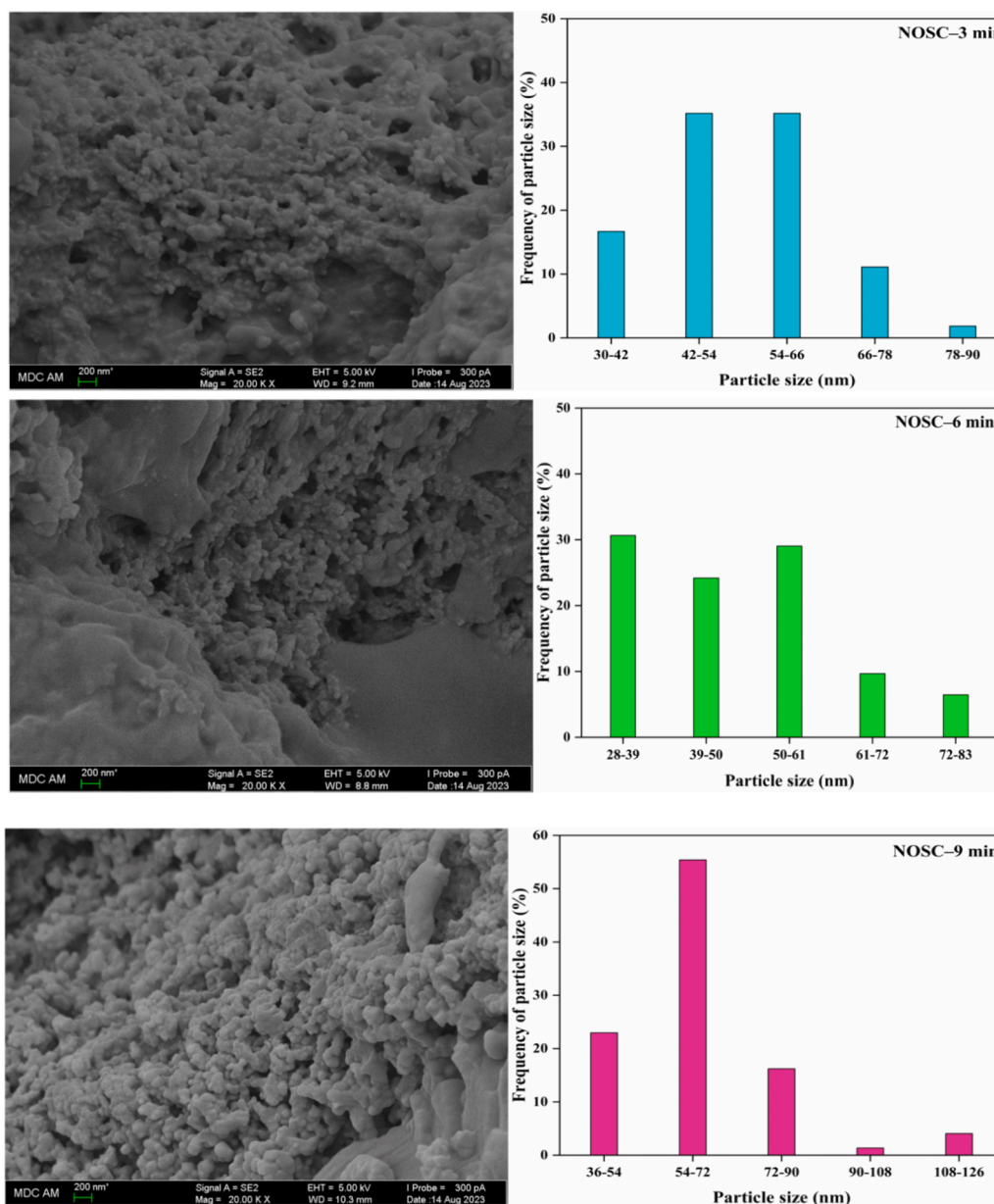**Fig. 8.** EDX curves of NOSC after EM heating treatment at different times.

Fig. 7. SEM images and particle size frequency of NOSC after EM heating treatment at different times.
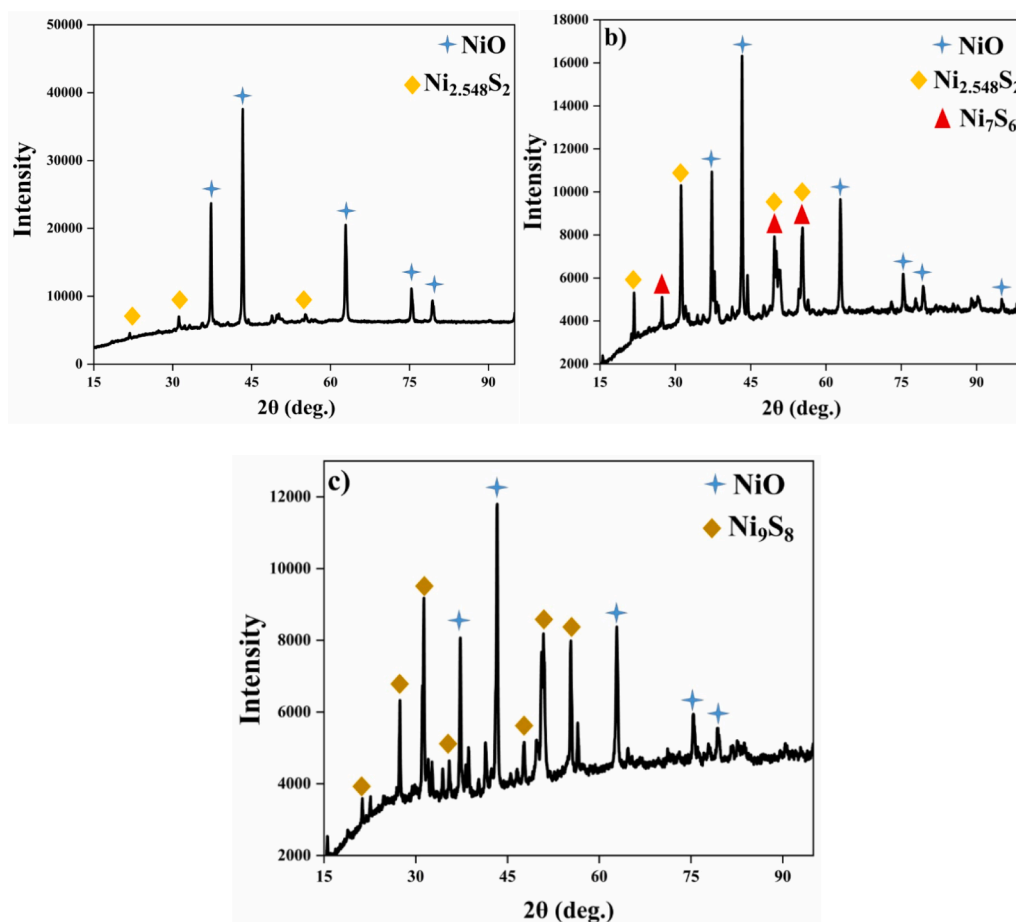
Fig. 9. XRD patterns of solids remaining after EM heating at 3 (a), 6 (b), and 9 (c) minutes.

desulfurization of ACO during the EM heating process. It is interesting that with increasing treatment time, the desulfurization process also showed an increasing trend. This phenomenon can be related to two factors, which are the increase of catalyst activity and the successive failure of weak C–S bonds. As shown in Fig. 10, increasing the temperature caused the thermal decomposition of NOSC during the process. The formation of nickel oxide is one of the side products of this decomposition. In the continuation of the reactions, NiO forms Ni_xS_y in contact with the sulfur present in asphaltenes and thus produces free radicals. The free radicals produced are subsequently transferred to lighter parts. In addition, Ni_xS_y is an active form of cracking catalyst that causes the formation of unsaturated hydrocarbons, which indicate an

Fig. 10. NOSC performance during the EM process (Reproduced with permission from [38]. Copyright 2019 American Chemical Society.).

increase in the light fractions of the oil composition.

3.2.6. FT–IR study

Qualitative analysis of ACO and resin and asphaltene fractions after microwave irradiation in the presence of NOSC was studied by FT–IR spectroscopy. Employing FT–IR spectroscopy provides valuable insights into the structural changes of ACO and the analysis of functional groups following the EM heating process in a system containing NOSC [63,64]. The results are shown in Fig. 11 and Fig. S5.

Spectral coefficients including aliphatic (C_1), aromaticity (C_2), branching (C_3), condensation (C_4), oxidation degree (C_5) and sulfurization (C_6) were calculated in order to quantitatively investigate the structural changes with the separation of oil, resins and asphaltenes (Table. 4). Meanwhile, the calculation methods and indicators of each of the coefficients are explained in the supplementary information.

During EM heating in the absence of NOSC, the aliphatic nature of ACO and resin (C_1) and aromatic content (C_2) did not change significantly. On the contrary, with NOSC, the spectral coefficients of C_1 decreased and C_2 increased. This increase occurs significantly after the process, which is carried out by the cracking reactions of aliphatic elements and the condensation of aromatic structures through radical recombination processes. Moreover, increased oxidation levels (C_5) occur when carbon-heteroatom bonds undergo hydrolysis to form phenols and alcohols. This intensification of oxidation is indicative of oxidative cracking, which is supported by elemental composition analysis. In addition, the significant decrease in sulfur content (C_6) not only leads to the decomposition of sulfur compounds through C–S bonds, but also indicates the presence of −SO groups, the conversion of sulfides to sulfoxides. Furthermore, the data obtained for asphaltenes showed that the aliphatic content (C_1) increases with the decrease of branching (C_3)
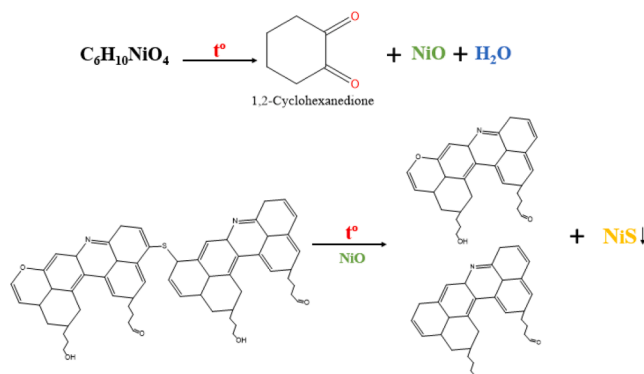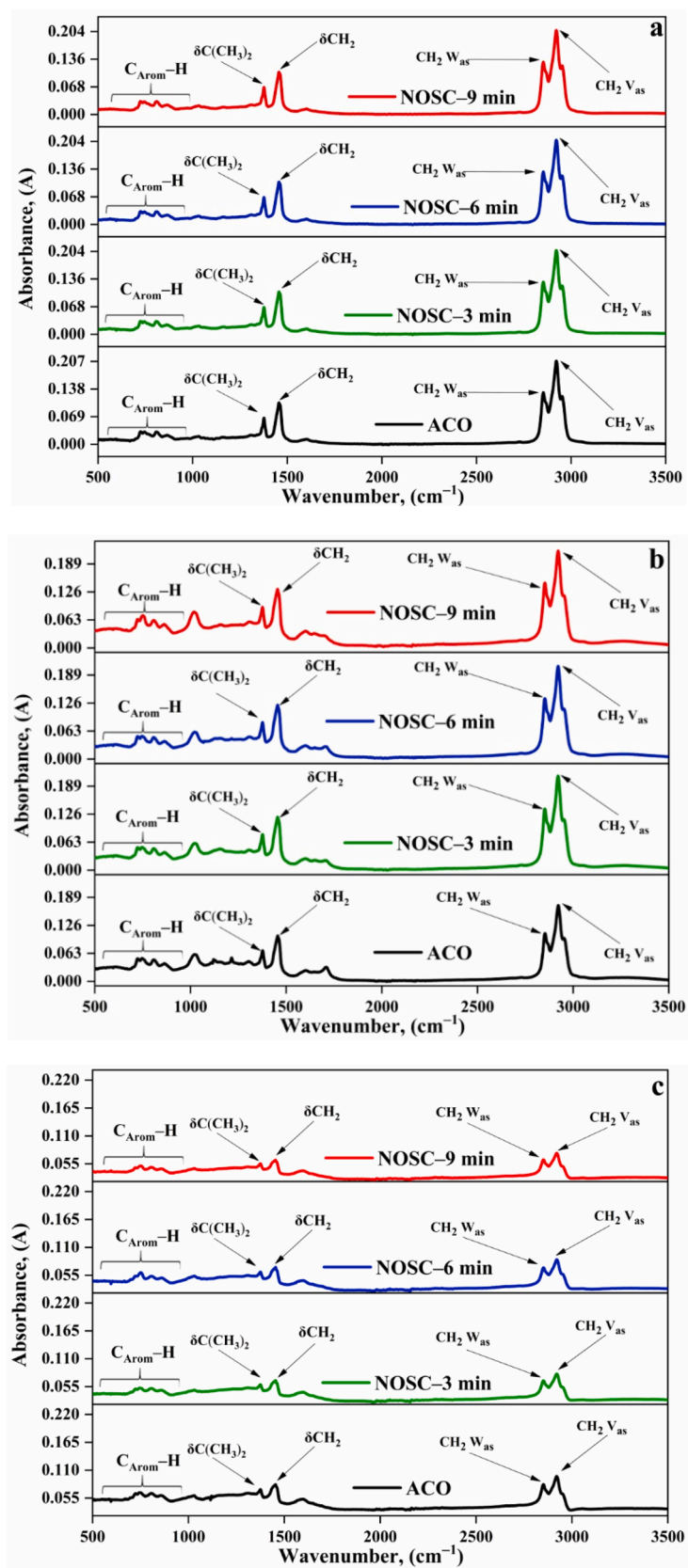
Fig. 11. FT–IR spectra of ACO (a), resin (b), and asphaltene (c) fractions under EM heating with NOSC systems at different times.

Table 4

FT–IR spectral coefficients of ACO, resin, and asphaltene fractions before and after EM heating treatment with NOSC systems at different times.
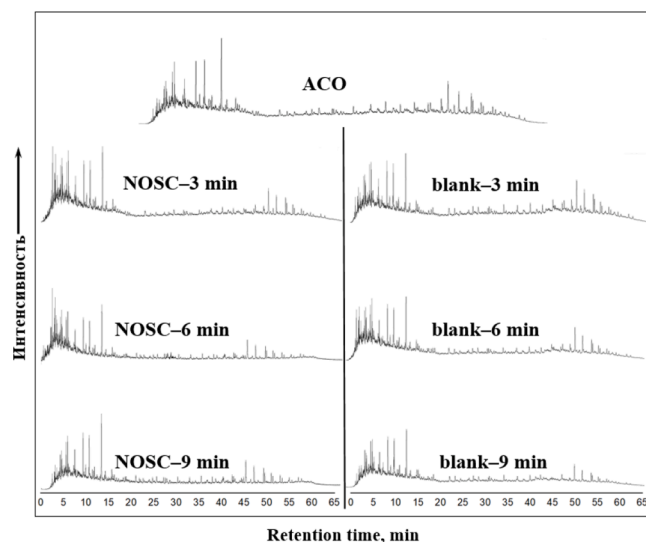
coefficient	Samples	C_1	C_2	C_3	C_4	C_5	C_6
Oil	ACO	0.82	0.15	1.61	0.23	3.25	1.59
	blank–3 min	0.82	0.15	1.65	0.24	3.65	1.59
	blank–6 min	0.82	0.15	1.63	0.25	3.40	1.59
	blank–9 min	0.81	0.15	1.70	0.25	3.36	1.58
	NOSC–3 min	0.77	0.15	1.75	0.25	4.04	1.51
	NOSC–6 min	0.78	0.15	1.77	0.25	3.73	1.55
	NOSC–9 min	0.75	0.16	1.76	0.25	3.96	1.55
Resins	ACO	0.42	0.21	1.18	0.18	1.31	2.77
	blank–3 min	0.44	0.21	1.22	0.18	1.10	2.56
	blank–6 min	0.40	0.23	1.22	0.21	1.26	2.54
	blank–9 min	0.45	0.21	1.24	0.20	1.28	2.36
	NOSC–3 min	0.40	0.23	1.27	0.27	0.92	2.21
	NOSC–6 min	0.45	0.22	1.38	0.29	0.84	2.27
	NOSC–9 min	0.35	0.26	1.27	0.31	0.72	2.06
Asphaltenes	ACO	1.54	0.40	1.05	0.42	0.74	1.13
	blank–3 min	1.53	0.40	1.06	0.42	0.73	1.12
	blank–6 min	1.56	0.41	1.06	0.42	0.73	1.12
	blank–9 min	1.53	0.41	1.10	0.42	0.74	1.12
	NOSC–3 min	1.52	0.42	1.10	0.44	0.72	1.10
	NOSC–6 min	1.58	0.40	1.80	0.41	0.73	1.20
	NOSC–9 min	1.51	0.42	1.10	0.41	0.74	1.11

due to the condensation process of asphaltene molecules. The reduction of the sulfurization coefficient in the resin (C_6) indicates a reduction in the concentration of sulfur-containing hydrocarbons, which can be consistent with the formation of Ni_x-S_y [65–67].
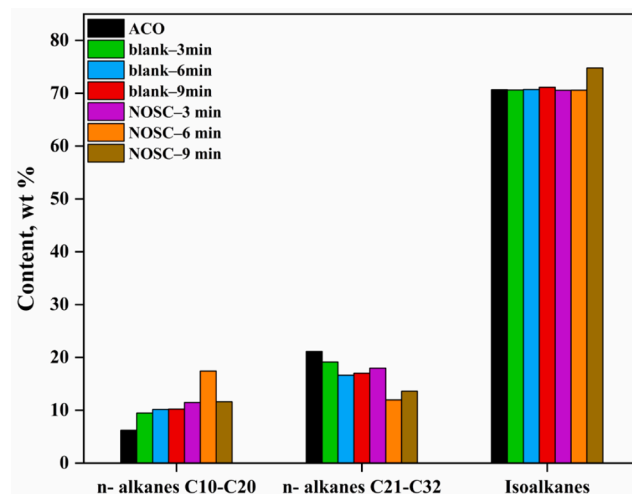
3.2.7. GC–MS study

In order to analyze the saturated fractions of ACO before and after the EM heating process, GC–MS analysis was performed and the relevant results are presented in Figs. 12, 13 and 14.

As shown in Fig. 13, the content of n-C_{10}–C_{15} increased from 6.19 wt % to 17.43 wt% during 6 min of EM heating in the presence of NOSC. In addition, the content of n-C_{26}–C_{32} was reduced compared to ACO in all samples. It is interesting that in 6 min the amount of these compounds is reduced by two times. On the contrary, except for NOSC–9 min, no significant change in isoalkanes content was observed in other samples. It should be noted that, the configuration of the naphthenic hump changes, reflecting branched alkanes that cannot be separated on the chromatographic column. Therefore, the intensity of the left part of the hump, corresponding to branched alkanes of lower molecular weight,

Fig. 13. The contents of n-alkanes before and after microwave treatment with and without NOSC at different times.

increases. This phenomenon indicates the degradation of large asphaltene molecules that contain alkyl substituents. During the EM heating process, an oxidation–reduction reaction occurs, which helps to weaken the bonds, thereby accelerating the degradation process of the asphaltene bundles [68,69]. The change in the total content of saturated hydrocarbons is shown in Fig. 14.

The sample treated for 9 min containing the NOSC showed the maximum change of alkanes by 20 %. Obviously, the content of cycloalkanes also changes depending on the duration of microwave exposure, so that for NOSC–6 min, the content of cycloalkanes increases twice, and the content of hopanes and homohopanes decreases almost proportionally. Isoalkanes are more easily oxidized than the corresponding n-alkanes, so during the chemical oxidation of ACO, the amount of iso-alkanes decreased. In light oils, C_{10}–C_{18} n-alkanes are usually present in maximum concentration. In heavy oils, the maximum distribution of n-alkanes is shifted to the C_{26}–C_{32} region and higher. during the analysis the content of gopans and homogopans should not be forgotten, because the reduction of these groups is evidence of a deep degradation in the composition of the oil [70]. It should be noted that these changes might be the result of the combined action of the catalyst and the microwave field.

The results related to the composition of aromatic fractions are presented in Figs. 15, 16, 17 and 18. As can be seen, Fig. 15 indicates the chromatogram of aromatic fractions based on total ion current and different ions for the most important aromatic compounds.

Significant changes occurred in the ratio between C_{10}–C_{18} and C_{19}–C_{27} alkylbenzenes, which is particularly noticeable for NOSC–6 min (Fig. 16). It is predicated that, the simultaneous effect of the presence of NOSC and the microwave field causes higher molecular weight alkylbenzenes to be destroyed to form lower molecular weight alkylbenzenes and approximately C_{10}–C_{12} alkane. This correlates with data on the content of typical alkanes in saturated hydrocarbons. A similar phenomenon was found for similar conditions of aquathermolysis of high molecular weight paraffins in ACO [71]. The maximum degree of alkylbenzene formation with low molecular weight was observed for NOSC–6 min. The increase in the content of light alkylbenzenes in NOSC–6 min compared to blank–6 min can be a reason for the acceptable performance of the NOSC in improving the quality of heavy oil during EM heating. Moreover, minor changes are observed in the naphthalene content (Fig. 17). The ratio between $C_{13}H_{14}$ and $C_{14}H_{16}$ changed after EM heating with NOSC system. This process is probably the result of degradation of resins and asphaltenes.

Electron withdrawing functional groups cause the instability of weak aliphatic disulfide bonds, which results in the degradation of
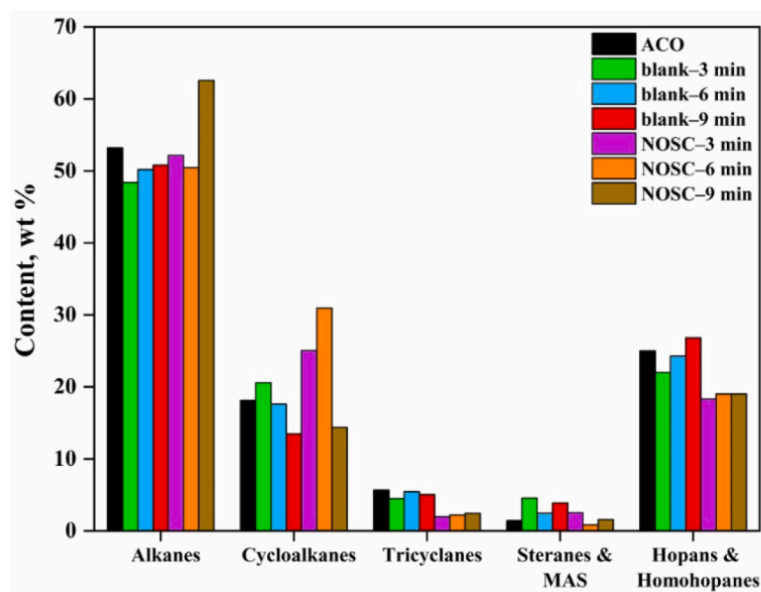

Fig. 12. Chromatograms of the saturated fraction of ACO after EM heating (with and without NOSC) at different times.

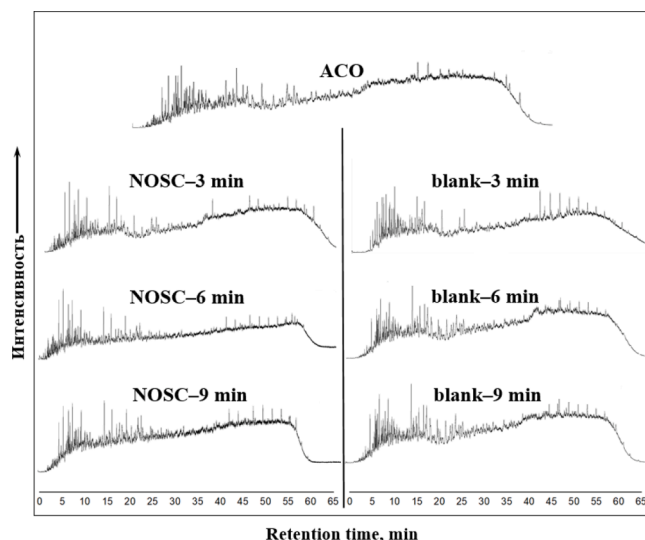**Fig. 14.** The composition of saturated hydrocarbons under EM heating with and without NOSC at different times.

Fig. 15. Chromatograms of the aromatic fraction of ACO after microwave treatment with and without NOSC at 3, 6 and 9 min.

Fig. 16. The contents of alkylbenzenes before and after microwave treatment with NOSC.

asphaltenes [72]. The result of the destruction of resins and asphaltenes is noticeable changes for other aromatic hydrocarbons. Mainly high-molecular ones, like, tetra-hydrophenanthrene, tetra-methylphenanthrene, and dimethylphenanthrene (Fig. 18).

Dibenzothiophenes content was reduced compared to ACO for all samples. Moreover, for the NOSC–6 min sample, the reduction degree of dibenzothiophenes is maximum and the highest increase in phenanthrene content was seen for NOSC–9 min, which seems that exposure to microwave radiation along with the catalyst facilitated the conversion of benzothiophenes to phenanthrenes.

3.3. Technology implementation schematic

Always in the research conducted in the field of electromagnetic heating, presenting an application plan on a field scale has been raised as a challenging issue [73]. A schematic design as a proposed method was presented in Fig. 19. The different parts that are numbered in the figure are as follows.
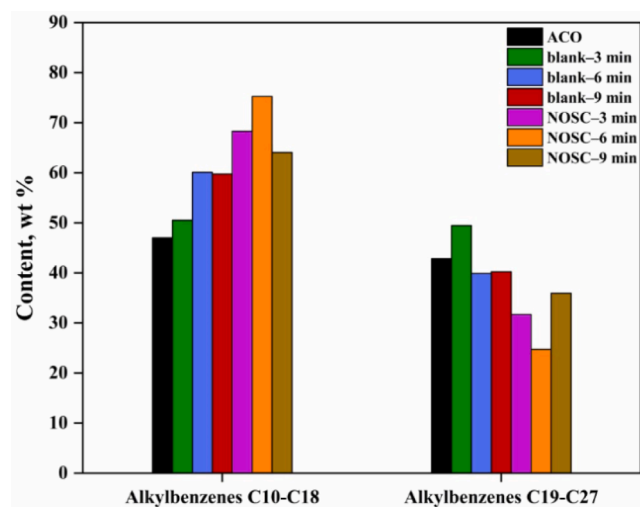
1) Power supply and automation equipment, 2) Tanker containing catalyst precursor, 3) Injection well, 4) Dispersed catalyst particles, 5) Magnetron, 6) Microwave radiation, 7) Temperature controller, 8) Hydraulic fractures and 9) Production well.

It should be noted that, in the first step, to intensify and increase the coverage of the formation, an oil-soluble precursor is transferred into the tank by the pump (As a suspension or through steam). Then, according to the physical and geological conditions of the tank, the location of the magnetrons and their number will be determined (probably between 5 and 15 pieces). The used power is at least 90 kW and the radiation frequency is 2.45 GHz. It is worth mentioning that by using the temperature control device, the intensity of the oil conversion process and formation heating in the well and the adjacent space can be analyzed and by changing the supply voltage, the temperature of the formation can be controlled within the required range. According to the investigation of the conditions of the Ashalcha heavy crude oil field (ACO) of the Republic of Tatarstan (Russia), the treatment period was predicted to be about 15 days.
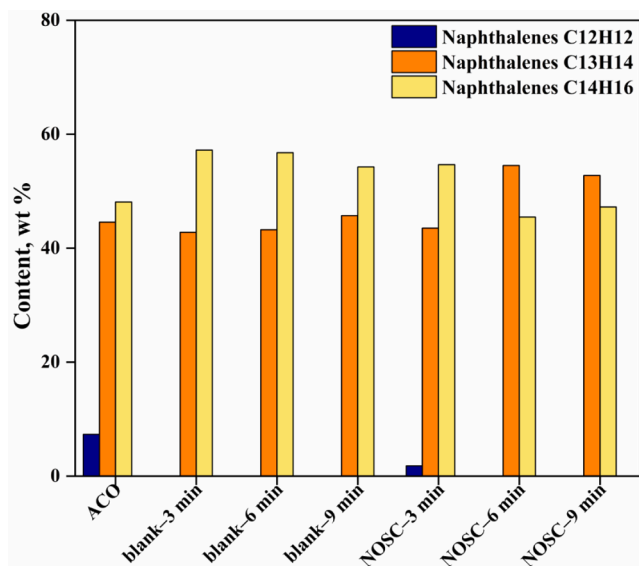
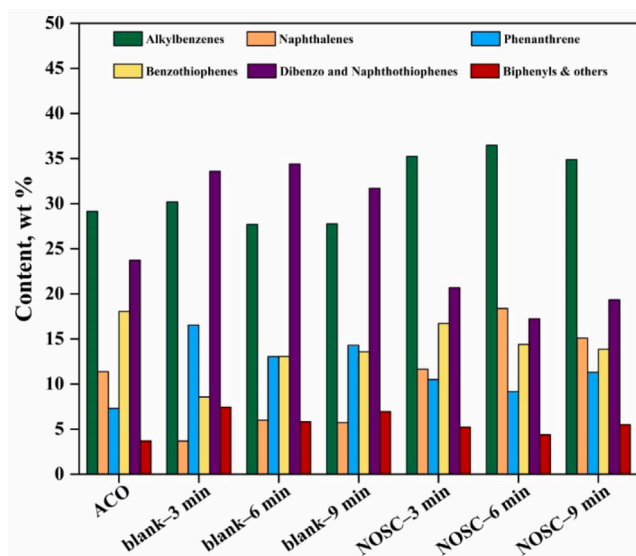**Fig. 17.** The contents of naphthalenes before and after microwave treatment.

Fig. 18. The relative content of various aromatic hydrocarbons before and after microwave treatment with NOSC.
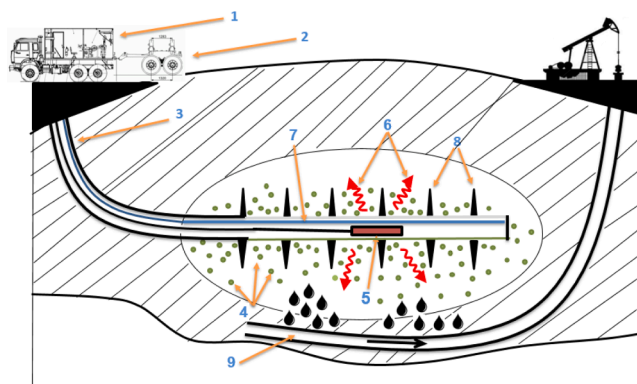

Fig. 19. Schematic diagram of formation processing under EM heating.

4. Conclusion

This paper investigated the optimization of heavy oil recovery using oil-soluble catalyst precursor under EM heating. So far, there has been no study on the integration of EM technology and this type of catalysts. The effect of NOSC and polar compounds (asphaltenenes and resins) due to their high ability to absorb microwave radiation cause an increasing point in temperature, which greatly increase the possibility of breaking and cracking of heavy hydrocarbons. In order that, results of SARA analysis for NOSC–9 min showed 42.4 wt% decrease in heavy compounds content (asphaltenes and resins) and 26.8 % increase in light compounds content (saturates and aromatics). The highest decrease in viscosity related to NOSC-9 min compared to ACO and blank samples. In the elemental analysis, destructive desulfurization and hydrogenation of compounds with high molecular weight (asphaltenes and resins) can be clearly seen, in the NOSC–9 min sample, the percentage of sulfur diminished from 5.77 wt% to 4.6 wt% and the ratio of H/C from 1.56 to 1.7 has changed. It should be noted that sulfur, which is present in crude oil compounds, has shown a high potential in absorbing microwave radiation. Therefore, this issue can cause the sulfur removal during the cracking of ACO compounds. Moreover, the GC–MS study showed that, the use of NOSC in all 3 time periods allowed the reduction of the concentration of polycyclic alkanes with high molecular weight and the increase of naphthalenes and alkylbenzenes in the ACO composition. In general, the obtained results can introduce the use of oil-soluble catalysts precursors in improving the efficiency of electromagnetic heating as a promising solution. Of course, this technology needs more in-depth and comprehensive research.

CRediT authorship contribution statement

Arash Tajik: Writing – review & editing, Writing – original draft, Validation, Supervision, Resources, Conceptualization. **Temurali Kholmurodov:** Writing – original draft, Validation, Formal analysis. **Yasser I. I. Abdelsalam:** Investigation, Formal analysis. **Nafis A. Nazimov:** Validation, Data curation. **Alexey V. Vakhin:** Supervision, Resources, Data curation.

Declaration of competing interest

The authors declare that they have no known competing financial interests or personal relationships that could have appeared to influence the work reported in this paper.

Data availability

No data was used for the research described in the article.

Appendix A. Supplementary data

Supplementary data to this article can be found online at https://doi.org/10.1016/j.fuel.2024.133043.

References

[1] Owusu PA, Asumadu-Sarkodie S. A review of renewable energy sources, sustainability issues and climate change mitigation. Cogent Eng 2016;3:1167990.
[2] Deshmukh MKG, Sameeroddin M, Abdul D, Sattar MA. Renewable energy in the 21st century: A review. Mater Today Proc 2023;80:1756–9.

[3] Kholmurodov T, Mirzaev O, Affane B, Tajik A, Romanova K, Galyametdinov Y, et al. Thermochemical Upgrading of Heavy Crude Oil in Reservoir Conditions. Processes 2023;11:2156.

[4] Gates ID, Wang J, Gates TD, Su Y, Kannaiyan R, Luo R. Heavy oil and extra heavy oil (bitumen) recovery. Recover. Improv.: Elsevier; 2023. p. 533–62.

[5] Hein FJ. Geology of bitumen and heavy oil: An overview. J Pet Sci Eng 2017;154:551–63.

[6] Shah A, Fishwick R, Wood J, Leeke G, Rigby S, Greaves M. A review of novel techniques for heavy oil and bitumen extraction and upgrading. Energy Environ Sci 2010;3:700–14. https://doi.org/10.1039/B918960B.

[7] Ahmadi M, Chen Z. Challenges and future of chemical assisted heavy oil recovery processes. Adv Colloid Interface Sci 2020;275:102081. https://doi.org/10.1016/J.CIS.2019.102081.

[8] Kholmurodov T, Vakhin A, ALIEV F, Galyametdinov Y, Mirzayev O, Tajik A, et al. Influence of Anionic and Amphoteric Surfactants on Heavy Oil Upgrading Performance with Nickel Tallate under Steam Injection Processes. Ind Eng Chem Res n.d.;62:10277–89. Doi: 10.1021/acs.iecr.3c01131.

[9] Guo K, Li H, Yu Z. In-situ heavy and extra-heavy oil recovery: A review. Fuel 2016;185:886–902.

[10] Ali SMF, Thomas S. The promise and problems of enhanced oil recovery methods. J Can Pet Technol 1996;35.

[11] Bera A, Babadagli T. Status of electromagnetic heating for enhanced heavy oil/bitumen recovery and future prospects: A review. Appl Energy 2015;151:206–26.

[12] Sherratt J, Sharifi Haddad A, Rafati R. Hot solvent-assisted gravity drainage in naturally fractured heavy oil reservoirs: A new model and approach to determine optimal solvent injection temperature. Ind Eng Chem Res 2018;57:3043–58.

[13] Chhetri AB, Islam MR. A critical review of electromagnetic heating for enhanced oil recovery. Pet Sci Technol 2008;26:1619–31.

[14] Dong X, Liu H, Chen Z, Wu K, Lu N, Zhang Q. Enhanced oil recovery techniques for heavy oil and oilsands reservoirs after steam injection. Appl Energy 2019;239:1190–211.

[15] Ritchey HW. Radiation heating: USA Patent Application 1956.

[16] Kovaleva L, Davletbaev A, Babadagli T, Stepanova Z. Effects of electrical and radio-frequency electromagnetic heating on the mass-transfer process during miscible injection for heavy-oil recovery. Energy Fuel 2011;25:482–6.

[17] Taheri-Shakib J, Shekarifard A, Naderi H. Experimental investigation of comparing electromagnetic and conventional heating effects on the unconventional oil (heavy oil) properties: Based on heating time and upgrading. Fuel 2018;228:243–53.

[18] Vakhin AV, Khelkhal MA, Tajik A, Gafurov MR, Morozov OG, Nasybullin AR, et al. The role of nanodispersed catalysts in microwave application during the development of unconventional hydrocarbon reserves: A review of potential applications. Processes 2021;9:1–20. https://doi.org/10.3390/pr9030420.

[19] Taheri-Shakib J, Kantzas A. A comprehensive review of microwave application on the oil shale: Prospects for shale oil production. Fuel 2021;305:121519.

[20] Li S-L, He J-H, Li Z, Lu J-H, Liu B-W, Fu T, et al. A sponge heated by electromagnetic induction and solar energy for quick, efficient, and safe cleanup of high-viscosity crude oil spills. J Hazard Mater 2022;436:129272.

[21] Pu W, He M, Yang X, Liu R, Shen C. Experimental study on the key influencing factors of phase inversion and stability of heavy oil emulsion: Asphaltene, resin and petroleum acid. Fuel 2022;311:122631.

[22] Ghanavati M, Shojaei M-J, Sa ar. Effects of asphaltene content and temperature on viscosity of Iranian heavy crude oil: experimental and modeling study. Energy Fuel 2013;27:7217–32.

[23] Zhang Y, Adam M, Hart A, Wood J, Rigby SP, Robinson JP. Impact of oil composition on microwave heating behavior of heavy oils. Energy Fuel 2018;32:1592–9.

[24] Karami S, Dehaghani AHS. A molecular insight into cracking of the asphaltene hydrocarbons by using microwave radiation in the presence of the nanoparticles acting as catalyst. J Mol Liq 2022;364:120026.

[25] Mutyala S, Fairbridge C, Paré JRJ, Bélanger JMR, Ng S, Hawkins R. Microwave applications to oil sands and petroleum: A review. Fuel Process Technol 2010;91:127–35.

[26] Tajik A, Vakhin AV, Nazimov NA, Mirzayev O, Latypov RR, Gafurov MR. Investigating the effect of microwave radiation at different frequencies on improving the quality of heavy oil. Fuel 2024;375:132547. https://doi.org/10.1016/j.fuel.2024.132547.

[27] Hanyong L, Kexin C, Ling J, Leilei W, Bo Y. Experimental study on the viscosity reduction of heavy oil with nano-catalyst by microwave heating under low reaction temperature. J Pet Sci Eng 2018;170:374–82.

[28] Sabet SA, Omidkhah M, Jafari A. Viscosity reduction of extra-heavy crude oil using nanocatalysts. Korean J Chem Eng 2022;39:1207–14.

[29] Hashemi R, Nassar NN, Almao. Nanoparticle technology for heavy oil in-situ upgrading and recovery enhancement: Opportunities and challenges. Appl Energy 2014;133:374–87.

[30] Medina OE, Olmos C, Lopera SH, Cortés FB, Franco CA. Nanotechnology applied to thermal enhanced oil recovery processes: A review. Energies 2019;12:4671.

[31] Shi H, Mao Z, Ran L, Ru C, Guo S, Dong H. Heavy oil viscosity reduction through aquathermolysis catalyzed by Ni20 (NiO) 80 nanocatalyst. Fuel Process Technol 2023;250:107911.

[32] Li H, Gao H, Zhao X, Xia Z, Yu B, Sun D. Experimental study on viscosity reduction of heavy oil with water content by synergistic effect of microwave and nano-catalyst. J Pet Sci Eng 2022;208:109271.

[33] Hamedi Shokrlu Y, Babadagli T. In-Situ Upgrading of Heavy Oil/Bitumen During Steam Injection by Use of Metal Nanoparticles: A Study on In-Situ Catalysis and Catalyst Transportation. SPE Reserv Eval Eng 2013;16:333–44. https://doi.org/10.2118/146661-PA.

[34] Li K, Hou B, Wang L, Cui Y. Application of carbon nanocatalysts in upgrading heavy crude oil assisted with microwave heating. Nano Lett 2014;14:3002–8.

[35] Vakhin AV, Khelkhal MA, Mukhamatdinov II, Mukhamatdinova RE, Tajik A, Slavkina OV, et al. Changes in Heavy Oil Saturates and Aromatics in the Presence of Microwave Radiation and Iron-Based Nanoparticles. Catalysts 2022;12:514.

[36] Taheri-Shakib J, Shekarifard A, Naderi H. Heavy crude oil upgrading using nanoparticles by applying electromagnetic technique. Fuel 2018;232:704–11.

[37] Simao A, Domínguez-Álvarez E, Yuan C, Suwaid MA, Varfolomeev MA, Ancheyta J, et al. On the use of metallic nanoparticulated catalysts for in-situ oil upgrading. Fuel 2022;313:122677.

[38] Al-Attas TA, Ali SA, Zahir MH, Xiong Q, Al-Bogami SA, Malaibari ZO, et al. Recent advances in heavy oil upgrading using dispersed catalysts. Energy Fuel 2019;33:7917–49.

[39] Saifullin ER, Mehrabi-Kalajahi S, Yuan C, Varfolomeev MA, Rodionov NO, Talipov S, et al. Catalytic combustion of heavy crude oil by oil-dispersed copper-based catalysts: Effect of different organic ligands. Fuel 2022;316:123335.

[40] Farhadian A, Khelkhal MA, Tajik A, Lapuk S, Rezaeisadat M, Eskin A, et al. Effect of Ligand Structure on the Kinetics of Heavy Oil Oxidation: Toward Biobased Oil-Soluble Catalytic Systems for Enhanced Oil Recovery. Ind Eng Chem Res n.d.;60:14713–27. Doi: 10.1021/acs.iecr.1c03276.

[41] Tajik A, Farhadian A, Khelkhal MA, Rezaeisadat M, Petrov SM, Eskin AA, et al. Sunflower oil as renewable biomass source to develop highly effective oil-soluble catalysts for in-situ combustion of heavy oil. Chem Eng J 2023;453. https://doi.org/10.1016/j.cej.2022.139813.

[42] Kholmurodov T, Tajik A, Farhadian A, Mirzayev O, Tahay P, Vakhin AV, et al. Development of a simple and efficient oil-soluble nanocatalytic system for aquathermolysis upgrading of heavy crude oil. Fuel 2023;353:129223.

[43] Fan Z, Zhao F, Wang J, Gong Y. Upgrading and viscosity reduction of super heavy oil by aqua-thermolysis with hydrogen donor. J Fuel Chem Technol 2006;34:315.

[44] Suwaid MA, Varfolomeev MA, Al-Muntaser AA, Yuan C, Starshinova VL, Zinnatullin A, et al. In-situ catalytic upgrading of heavy oil using oil-soluble transition metal-based catalysts. Fuel 2020;281:118753.

[45] Vakhin AV, Aliev FA, Mukhamatdinov II, Sitnov SA, Sharifullin AV, Kudryashov SI, et al. Catalytic aquathermolysis of boca de jaruco heavy oil with nickel-based oil-soluble catalyst. Processes 2020;8:532.

[46] Yuan C, Mehrabi-Kalajahi SS, Sadikov K, Varfolomeev MA, Emelianov DA, Rodionov NO, et al. Potential of copper-based oil soluble catalyst for improving efficiency of in-situ combustion process: catalytic combustion, catalytic in-situ oil upgrading, and increased oil recovery. SPE Kuwait Oil Gas Show Conf., SPE; 2019, p. D033S013R006.

[47] Sitnov SA, Mukhamatdinov II, Vakhin AV, Ivanova AG, Voronina EV. Composition of aquathermolysis catalysts forming in situ from oil-soluble catalyst precursor mixtures. J Pet Sci Eng 2018;169:44–50.

[48] Qin WL, Xiao ZL. The Researches on Upgrading of Heavy Crude Oil by Catalytic Aquathermolysis Treatment Using a New Oil-Soluble Catalyst. Adv Mater Res 2013;608–609:1428–32. https://doi.org/10.4028/www.scientific.net/AMR.608-609.1428.

[49] Smith BC. The C═O bond, part III: Carboxylic acids. Spectroscopy 2018;33:14–20.

[50] Bronstein LM, Huang X, Retrum J, Schmucker A, Pink M, Stein BD, et al. Influence of iron oleate complex structure on iron oxide nanoparticle formation. Chem Mater 2007;19:3624–32.

[51] Hemath M, Mavinkere Rangappa S, Kushvaha V, Dhakal HN, Siengchin S. A comprehensive review on mechanical, electromagnetic radiation shielding, and thermal conductivity of fibers/inorganic fillers reinforced hybrid polymer composites. Polym Compos 2020;41:3940–65.

[52] Bradhurst DH, Worner HK. Evaluation of oil produced from the microwave retorting of Australian shales. Fuel 1996;75:285–8.

[53] Monsef-Mirzai P, Ravindran M, McWhinnie WR, Burchill P. Rapid microwave pyrolysis of coal: Methodology and examination of the residual and volatile phases. Fuel 1995;74:20–7.

[54] Taheri-Shakib J, Shekarifard A, Naderi H. The experimental study of effect of microwave heating time on the heavy oil properties: Prospects for heavy oil upgrading. J Anal Appl Pyrolysis 2017;128:176–86.

[55] Tao R, Xu X. Reducing the viscosity of crude oil by pulsed electric or magnetic field. Energy Fuel 2006;20:2046–51.

[56] Shang H, Zhang H, Du W, Liu Z. Development of microwave assisted oxidative desulfurization of petroleum oils: A review. J Ind Eng Chem 2013;19:1426–32.

[57] Leadbeater NE, Khan MR. Microwave-promoted desulfurization of heavy and sulfur-containing crude oil. Energy Fuel 2008;22:1836–9.

[58] Betiha MA, ElMetwally AE, Al-Sabagh AM, Mahmoud T. Catalytic aquathermolysis for altering the rheology of asphaltic crude oil using ionic liquid modified magnetic MWCNT. Energy Fuel 2020;34:11353–64.

[59] Sánchez-Delgado RA. Breaking CS bonds with transition metal complexes. A review of molecular approaches to the study of the mechanisms of the hydrodesulfurization reaction. J Mol Catal 1994;86:287–307. https://doi.org/10.1016/0304-5102(93)E0159-E.

[60] Ma Y-Y, Fan X, Mo W-L, Li G-S, Ma F-Y, Wei X-Y. Catalytic hydrogenation and heteroatom removal for isopropanol soluble organic matter of Dongming lignite. Fuel Process Technol 2021;211:106589. https://doi.org/10.1016/j.fuproc.2020.106589.

[61] Li H, Wang Y, Qin S, Cao S, Yu B, Sun D. Study on Viscosity Reduction Mechanism for Offshore Heavy Oil Under the Synergistic Action of Nanocatalyst and Ultrasound. Offshore Technol Conf Asia 2020:D012S001R024. Doi: 10.4043/30398-MS.

[62] Sviridenko NN, Urazov KK. Catalytic upgrading of heavy oil from the Ashalchinskoye oilfield. Pet Sci Technol 2023;41:1918–33.

[63] Xiong P, Yang H, Wu P, Liao Y, Tan D, Ma Z, et al. Study on catalytic aquathermolysis of heavy oil by simple synthesis of highly dispersed nickel-loaded nitrogen-doped carbon catalysts. Mol Catal 2022;529:112528.

[64] Al-Muntaser AA, Varfolomeev MA, Suwaid MA, Feoktistov DA, Yuan C, Klimovitskii AE, et al. Hydrogen donating capacity of water in catalytic and non-catalytic aquathermolysis of extra-heavy oil: Deuterium tracing study. Fuel 2021; 283:118957.

[65] Smith BC. Infrared spectral interpretation: a systematic approach. CRC Press; 2018.

[66] Wong KC. Review of spectrometric identification of organic compounds 2015.

[67] Abdelsalam YII, Akhmetzyanova LA, Galiakhmetova LK, Baimukhametov GF, Davletshin RR, Dengaev AV, et al. The Catalytic Upgrading Performance of NiSO4 and FeSO4 in the Case of Ashal'cha Heavy Oil Reservoir. Processes 2023;11:2426.

[68] Shebl MA, Surdam RC. Redox reactions in hydrocarbon clastic reservoirs: experimental validation of this mechanism for porosity enhancement. Chem Geol 1996;132:103–17.

[69] Wittle JK, Bell CW. Electrochemical process for effecting redox-enhanced oil recovery 2005.

[70] Kholmurodov T, Khelkhal MA, Galyametdinov Y, Ayaz N, Tajik A, Sitnov SA, et al. Innovative dual injection technique of nonionic surfactants and catalysts to enhance heavy oil conversion via aquathermolysis. Fuel 2024;366:131274.

[71] Mukhamatdinov II, Ali MON, Mukhamatdinova RE, Affane B, Vakhin AV, Tsvetkov SV, et al. Optimization of thermal steam treatment technology applied to Strelovskoye field using aquathermolysis catalysts. Fuel 2024;359:130389.

[72] Vakhin AV, Mukhamatdinov II, Sitnov SA, Mukhamatdinova RE, Simakov IO, Nikitina EA, et al. Catalytic Activity of Nickel and Iron Sulfides in the Degradation of Resins and Asphaltenes of High-Viscosity Oil in the Presence of Carbonate Rock Under Hydrothermal Conditions. Kinet Catal 2022;63:569–76.

[73] Mukhametshina A, Martynova E. Electromagnetic heating of heavy oil and bitumen: a review of experimental studies and field applications. J Pet Eng 2013; 2013:476519.